Synthetic Metals 239 (2018) 22–28

Contents lists available at ScienceDirect

Synthetic Metals

journal homepage: www.elsevier.com/locate/synmet

Impact of Ag@SiO$_2$ core-shell nanoparticles on the photoelectric current of plasmonic inverted organic solar cells

Kekeli N'Konou[a], Malika Chalh[b], Virginie Monnier[c], Nicholas P. Blanchard[d], Yann Chevolot[c], Bruno Lucas[b], Sylvain Vedraine[b], Philippe Torchio[a,*]

[a] Aix-Marseille Univ, IM2NP, CNRS-UMR 7334, Domaine Universitaire de Saint-Jérôme, Service 231, 13397, Marseille Cedex 20, France
[b] Université de Limoges, XLIM-CNRS 7252, 123 Avenue Albert Thomas, 87060, Limoges, France
[c] Université de Lyon, Institut des Nanotechnologies de Lyon UMR CNRS 5270, Ecole Centrale de Lyon, 36 Avenue Guy de Collongue, F-69134, Ecully, France
[d] Université de Lyon, Université Claude Bernard Lyon 1, CNRS, Institut Lumière Matière, F-69622, Villeurbanne, France

ARTICLE INFO

Keywords:
Ag@SiO2 core-shell nanospheres
Plasmonic solar cells
Absorption enhancement
Finite-difference time-domain method

ABSTRACT

We report on the influence of silver-silica core-shell nanoparticles (Ag@SiO$_2$ NPs) and bare silver nanoparticles (Ag NPs) on the photoelectric current of plasmonic inverted organic solar cells. The synthesized Ag@SiO$_2$ NPs are deposited on a zinc oxide layer. The optimized plasmonic devices concern the Ag@SiO$_2$ NPs with 5 nm shell thickness and present the highest short-circuit current density of 13.44 mA/cm^2, enhanced by 12% compared to the reference device. Such enhancements can mainly be attributed to the localized surface plasmon resonance and to the light scattering effect originating from Ag NPs and Ag@SiO$_2$ NPs. Finite-difference time-domain simulation reveals that a thin shell thickness facilitates the extension of a strong localized enhanced electromagnetic field in the active layer, as confirmed by measured and simulated optical absorption and photoluminescence measurements. Furthermore, AFM images present a well-distributed Ag@SiO$_2$ NPs array on the ZnO films, which contributes to such an improvement.

1. Introduction

During the past several years, plasmonic organic solar cells (OSCs) are widely studied due to the advantages of metallic nanoparticles embedded in OSCs which exploit the light scattering and the localized surface plasmon resonance (LSPR) effects for increasing light harvesting [1–3].

The plasmonic materials or metal nanoparticles (MNPs) such as silver [4,5], gold [6,7] or aluminum nanoparticles [8,9] are frequently used for their capability to enhance OSC devices photoelectric properties, which essentially originates from the enhancement in light absorption. Embedding solution-processed MNPs into OSCs is a promising method for increasing light harvesting because of the controllable optical properties, low-cost and compatibility with OSC fabrication technology.

The integration of MNPs in OSCs can excite LSPR, inducing an increase in light absorption, and then an improvement in exciton generation [10,11]. Several reviews related to plasmonic OSCs studies have reported that the performance (such as light absorption and power conversion efficiency (PCE)) of OSCs are improved by introducing metal nanostructures with different shapes, sizes and concentration into the different layers of OSCs, such as active layers [12–14], hole-transport layers (HTL) [15–17] and electron-transport layers (ETL) [18–20]. Choy and co-workers have investigated [21–24] the role of gold nanostars inserted between the HTL and the active layer of OSCs and proposed an explanation of the mechanisms involved in the performance enhancement. They ascribed the optical absorption enhancement in the active layer to the energy transfer induced by the excited plasmonic asymmetric modes. Furthermore, they observed that the near field distribution in the structure can reallocate the exciton generation regions. If the geometry is optimized, the plasmonic nanoparticles can lead to the favorable generation of excitons close to the interfacial layer that is particularly interesting when hole and electron mobilities differ by several orders of magnitude. This transfer of the exciton generation region from the middle of the active layer to close proximity of the HTL involves an increase in the transport path length of the electron-to-cathode while the transport path length of the hole-to-anode shortens. Li et al. [25] demonstrated that the incorporation of the mixed Ag nanomaterials of different shapes into the active layer can improve significantly the performance of OSCs in a conventional structure through plasmonic effect. Their theoretical and experimental studies revealed that a broadband resonance is achieved by the simultaneous

---

[*] Corresponding author.
E-mail address: philippe.torchio@univ-amu.fr (P. Torchio).

https://doi.org/10.1016/j.synthmet.2018.03.003
Received 11 October 2017; Received in revised form 18 January 2018; Accepted 3 March 2018

excitation of versatile plasmonic resonances depending on several parameters such as shape, size, polarization, low and high-order plasmonic resonances. However such improved performance with bare MNPs is not consistently observed in plasmonic OSCs. Choi et al. [26] reported that embedding bare Ag NPs in conventional OSCs lead to poor device performance and that exciton quenching from direct contact between the active layer and Ag NPs probably induces this deficient performance.

It has also been demonstrated that MNPs insulated by a dielectric shell, so called core-shell metal@dielectric nanoparticles, can lead to better photovoltaic performance than bare MNPs as the dielectric shell can prevent direct contact between the active layer and MNPs and consequently reduce charge recombination and exciton quenching losses at the metal surface [27,28]. Xu et al. [29] revealed that the thickness of the silica shell was a key parameter of core-shell metal@dielectric nanoparticles design and the incorporation of MNPs insulated by a thin silica shell in standard OSCs was able to enhance the device performance. In a previous study, we numerically demonstrated [30] that increasing silica shell thickness was detrimental for achieving an enhanced near-field effect around MNPs incorporated in the active layer and caused a considerable decrease of the optical absorption. A related experimental study on the influence of silica shell thickness on device performance in plasmonic OSC devices with Au-silica nanorods previously reported that a 5 nm-thick silica shell can greatly improve the photovoltaic performance and light absorption in the active layer while the use of silica shell thickness less than 2 nm will create incomplete encapsulation, leading to an exciton quenching at the surface of these Au-silica nanorods [31]. However, to our knowledge, no systematic study on the influence of silver-silica nanoparticles (Ag@SiO_2 NPs) on the optical and electrical properties of inverted OSCs has as yet been reported. In this study, we investigate the impact of Ag@SiO_2 NPs on the photoelectric current of plasmonic inverted OSCs by embedding bare Ag NPs and Ag@SiO_2 NPs on top of a zinc oxide (ZnO) layer. The choice of the position of these NPs inside the device is motivated by the fact that in another optical numerical study [32], we demonstrated that inverted plasmonic OSCs present 26% and 27% enhancement in short-circuit current density and optical absorption enhancement, respectively, when Ag@SiO_2 NPs are placed on top of the cathodic buffer layer.

2. Experimental details

2.1. Materials

Silver nitrate ($AgNO_3$), trisodium citrate, isopropanol, ethanol, polyvinylpyrrolidone with average molecular weight of 10 000 g/mol (PVP10), tetraethylorthosilicate (TEOS) and ammonia solution (30%) were purchased from Sigma-Aldrich. The ZnO nanoparticle solution was obtained from Genes'Ink, PEDOT:PSS (F010) was bought from Clevios. Poly(3-hexylthiophene) (P3HT) and 1-(3-methoxycarbonyl)-propyl-1-phenyl-(6,6)C_{61}(PCBM) were purchased from Rieke Metals and American Dye Source, respectively.

2.2. Synthesis of Ag and Ag@SiO_2 NPs

Ag NP dispersions were prepared from an $AgNO_3$ solution (9 mg of $AgNO_3$ powder dissolved in 49 mL of water) heated to reflux under magnetic stirring in the dark. Then, 1 mL of a 10 g/L trisodium citrate was rapidly injected into the $AgNO_3$ solution. After 1 h, a Ag NPs dispersion containing 3.3×10^{10} NPs/mL was obtained. Ag@SiO_2 NPs were prepared from 2 mL of the Ag NP dispersion (3.3×10^{10} NPs/mL) mixed with 50 mL of water and 75 μL of PVP10 solution (12.8 g/L). The reaction mixture was stirred for 24 h at room temperature. The PVP modified NPs were collected by centrifugation at 7600*g* for 5 min. Then, after supernatant removal, 8 μL of ammonia solution 30% and 70 μL of ethanol were added dropwise and under vigorous magnetic stirring. Addition of 0.2 μL of TEOS to the Ag NPs solutions leads to the formation of the silica shell with thicknesses around 5 nm. The reaction mixture was then stirred for another 1 h. The Ag@SiO_2 NPs were separated by centrifugation at 7600g for 5 min, and finally re-dispersed into 2 mL of water.

2.3. Plasmonic inverted OSC device fabrication

Deionized water, acetone, and isopropyl alcohol were used to clean the ITO-covered glass substrates (12×12 mm^2) under ultrasonication. The substrates were then blown dry using N_2 gas before being used. The ZnO NP solution was spin-coated (4000 rpm, 50 s) with a thickness of 20 nm and annealed at 130 °C for 10 min on a hot plate. The Ag NPs and Ag@SiO_2 NPs dispersions were spin-coated (1 000 rpm, 30 s) on the ZnO layer and transferred into a glove box, followed by annealing at 50 °C for 5 min to remove the solvent. 60 mg P3HT and 48 mg of $PC_{61}BM$ blend in 2 ml of 1,2-dichlorobenzene solution were prepared at least 24 h before use. P3HT:$PC_{61}BM$ blend solution was deposited by spin-coating (1200 rpm, 35 s) with a thickness of 250 nm. After a 2h solvent-annealing treatment in glove box at room temperature, PEDOT:PSS film was spin-coated (5000 rpm, 50 s). After transferring the substrate to a vacuum chamber, 150 nm-thick silver (Ag) layers were thermally evaporated at a pressure of 2×10^{-6} Torr through a shadow mask of 0.18 cm^2. The final device structure of the plasmonic inverted OSCs with a configuration of ITO/ZnO/Ag@SiO_2 NPs/P3HT:$PC_{61}BM$/PEDOT:PSS/Ag is shown in Fig. 1.

2.4. Device characterization

The surface morphology of the films was obtained by atomic force microscopy (CSI Nano-Observer AFM) while the transmission electron microscopy (TEM) images of Ag@SiO_2 NPs were obtained with a JEOL 2100HT microscope operated at 200 kV. For TEM studies, 2 μL of the diluted dispersion of nanoparticles was deposited onto a carbon holey grid (Ted Pella Inc.). Images were analyzed with ImageJ 1.46r software. Energy Dispersion X-Ray (EDX) spectroscopy line scans were obtained in scanning TEM mode using the same JEOL 2100HT. The LSPR effects of these Ag and Ag@SiO_2 NPs were simulated using Lumerical FDTD Solutions© software. The current density–voltage (J–V) curves were measured using a Keithley 2400 source under simulated AM1.5 solar irradiance at 100 mW/cm^2. The UV absorption spectra of multilayers were taken using a UV/Vis/near-IR spectrophotometer (Perkin Elmer Lambda 950). The absorption (A) was acquired from transmission (T) and reflection (R) by the equation: A = 1 − R − T. The photoluminescence spectra of P3HT:PCBM films was obtained using a Horiba Jobin Yvon iHR 320.

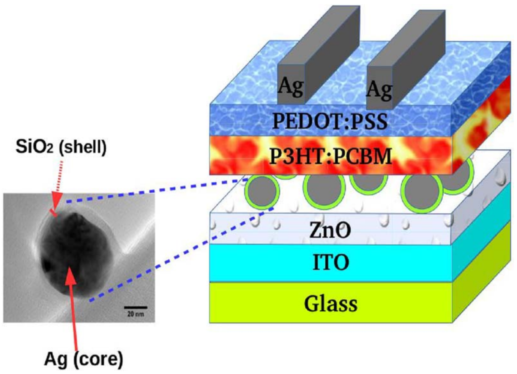

Fig. 1. Device structure of the plasmonic inverted OSCs.